

## X-RAY ABSORPTION BY WHIM IN THE SCULPTOR WALL

DAVID A. BUOTE<sup>1</sup>, LUCA ZAPPACOSTA<sup>1,2</sup>, TAOTAO FANG<sup>1</sup>, PHILIP J. HUMPHREY<sup>1</sup>,  
FABIO GASTALDELLO<sup>1,3,4</sup>, & GIANPIERO TAGLIAFERRI<sup>5</sup>

*Accepted for Publication in The Astrophysical Journal*

### ABSTRACT

We present *XMM* RGS and *Chandra* LETG observations of the blazar, H 2356-309, located behind the Sculptor Wall, a large-scale galaxy structure expected to harbor high-density Warm-Hot Intergalactic Medium (WHIM). Our simultaneous analysis of the RGS and LETG spectra yields a  $3\sigma$  detection of the crucial redshifted O VII  $K\alpha$  line with a column density ( $\gtrsim 10^{16}$  cm<sup>-2</sup>) consistent with similar large-scale structures produced in cosmological simulations. This represents the first detection of non-local WHIM from X-ray absorption studies where *XMM* and *Chandra* data are analyzed simultaneously and the absorber redshift is already known, thus providing robust evidence for the expected repository of the “missing baryons”.

*Subject headings:* X-rays: diffuse background — X-rays: galaxies: clusters — cosmology: observations  
— cosmology: diffuse radiation — galaxies: BL Lacertae objects: individual :  
H 2356-309

### 1. INTRODUCTION

At most 50% of the total baryonic matter in the nearby universe can be accounted for by the amount of luminous baryons revealed by observations of stellar light, narrow Ly $\alpha$  absorption systems, and X-ray emission from hot gas in galaxy clusters (e.g., Fukugita et al. 1998). Cosmological simulations predict that most of the “missing baryons” (30-50%) reside in low-density plasma in large-scale filamentary structures between galaxies (e.g., Cen & Ostriker 1999; Davé et al. 2001). The location and predicted temperature range ( $10^5 - 10^7$  K) of this plasma motivated its name as the “Warm-Hot Intergalactic Medium” (WHIM).

Ultraviolet observations of O VI absorption lines in background quasar spectra provided the first clear detection of the WHIM (e.g., Savage et al. 1998; Tripp et al. 2006, and references therein). The O VI lines probe lower temperature WHIM ( $\approx 10^5$  K), while most of the WHIM gas is expected to exist at higher temperatures observable only at X-ray wavelengths (e.g., Davé et al. 2001). Important evidence for WHIM in X-ray emission has been provided by, e.g., correlation studies of X-ray emission and galaxy positions in superclusters (e.g., Zappacosta et al. 2002, 2005) and by X-ray imaging studies of the highest density WHIM near massive clusters (e.g., Werner et al. 2008, and references therein).

Because of the difficulty in treating the foreground X-ray emission from the Milky Way, it is important to corroborate these detections with X-ray absorption-line studies which are largely insensitive to this issue. Typically, X-ray absorption studies focus on the O VII  $K\alpha$  line ( $\lambda = 21.6$  Å), because it is expected to be the strongest line at X-ray energies owing to the anticipated WHIM

temperature and the relatively high cosmic abundance of oxygen.

To date there is no detection of WHIM in X-ray absorption that is generally accepted by the astronomical community (e.g., Richter et al. 2008, and references therein). The case of Mkn 421 illustrates the problem. Nicastro et al. (2005) first reported highly significant detections of two absorption systems along the Mkn 421 sight line using a deep *Chandra* observation. But Kaastra et al. (2006) showed that the statistical significance of the lines reported by Nicastro et al. (2005) was greatly overestimated because the redshifts of the absorbers were not known *a priori*. Furthermore, a deeper *XMM* observation of Mkn 421 did not confirm the presence of the claimed absorption systems (Rasmussen et al. 2007).

To address these issues, we consider a different observational approach proposed by Kravtsov et al. (2002) and pioneered by Fujimoto et al. (2004) in their absorption study of the Virgo cluster. Rather than performing a so-called “blind” search for previously unknown intervening WHIM structures in front of the brightest background AGN, we perform a “targeted” search by choosing a region of sky that provides an optimal combination of known large-scale structure and a bright, intrinsically featureless, background source. Because the redshift of the foreground structure is known *a priori*, the statistical significance of a detected line is much higher than for a blind search. By focusing on large-scale structure, we should observe relatively high density WHIM, therefore aiding a detection. We restrict our study to background blazars because of their intrinsically featureless spectra compared to other AGN.

In this paper we present *XMM* and *Chandra* grating observations of the blazar H 2356-309 ( $z = 0.165$ ) located behind the Sculptor Wall (Figure 1), a southern super-structure filled with many groups and clusters of galaxies (da Costa et al. 1994). The part of the Sculptor Wall intercepted by the sight-line of H 2356-309 represents a redshift range of 0.028-0.032. Although the observations were designed as Targets-of-Opportunity to catch

<sup>1</sup> Department of Physics and Astronomy, University of California at Irvine, 4129 Frederick Reines Hall, Irvine, CA 92697-4575

<sup>2</sup> INAF - Osservatorio Astronomico di Trieste, Via Tiepolo 11, 34143 Trieste, Italy

<sup>3</sup> INAF - IASF Milano, Via E. Bassini 15, I-20133 Milano, Italy

<sup>4</sup> Occhialini Fellow

<sup>5</sup> INAF-Osservatorio Astronomico di Brera, Via Bianchi, 46, 23807 Merate, Italy

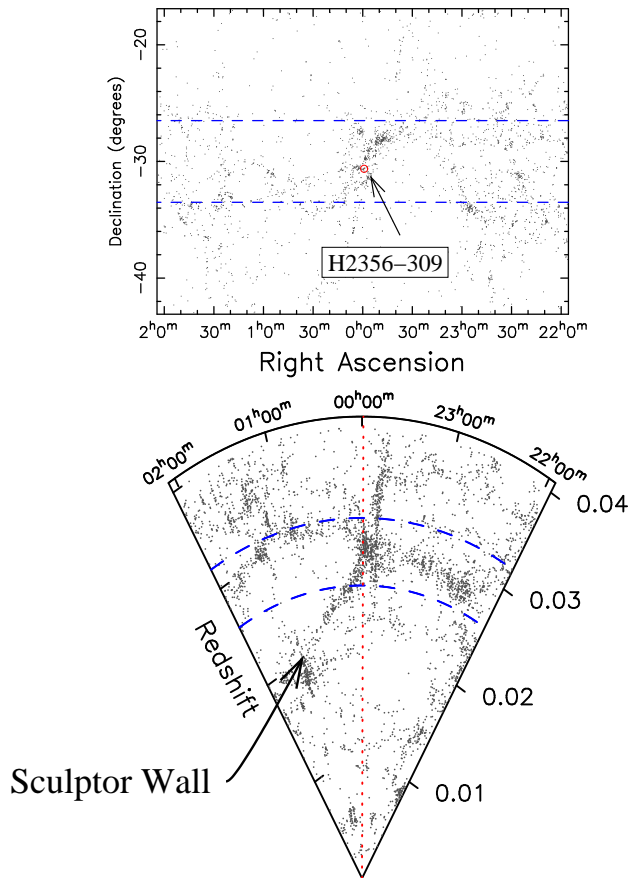


FIG. 1.— Sky map (top) and wedge diagram (bottom), each expressed in R.A., of the region of the Sculptor Wall where the blazar H 2356-309 is located. Galaxy redshifts are taken from NED. The (blue) dashed lines in the upper panel define the range of declination of the galaxies displayed in the lower panel. Conversely, the (blue) dashed lines in the lower panel define the redshift range of the points in the upper panel. The blazar line-of-sight is indicated by the (red) dotted line in the wedge diagram.

H 2356-309 in outburst, the apparent outbursts were not long enough to enable the follow-up (10-40 hours after triggering) to catch the blazar in a high state. The observations were performed four months apart because of different triggering criteria used for the different satellites.

Despite H 2356-309 being observed in its low state ( $\sim 10^{-11}$  erg cm $^{-2}$  s $^{-1}$  0.5-2.0 keV flux), we detected a candidate WHIM O VII resonance line in the Sculptor Wall from a simultaneous fit of the *XMM* and *Chandra* data. Although we examined other candidate lines from other parts of the spectra using all the *XMM* and *Chandra* data, here we present only the results for the O VII line because only for it do we achieve a detection of at least  $3\sigma$  significance.

The paper is organized as follows. In §2 we present the observations and describe the data preparation. The spectral fitting, modeling approach, and systematic errors are discussed in §3. We present our conclusions in §4.

## 2. OBSERVATIONS

On June 2, 2007 *XMM* observed H 2356-309 (ObsID 0504370701) for approximately 130 ks with the Reflec-

tion Grating Spectrometer (RGS) as the primary instrument. The RGS is comprised of two nominally identical sets of gratings, the RGS1 and RGS2. But due to the failure of one of the CCD chips early in the mission, the RGS2 lacks sensitivity over the energy range (20 – 24 Å) relevant for the O VII lines. Consequently, we focus on the RGS1 in this paper. We analyzed the RGS1 data with the most up-to-date *XMM-Newton* Science Analysis Software (SAS 8.0.0)<sup>6</sup> along with the latest calibration files.

We generated a light curve of the background events using CCD number 9; i.e., the CCD that is close to the optical axis and is most likely to be affected by the background flares. Inspection of the light curve does reveal a flare near the end of the observation, which we removed, resulting in a clean exposure of 126 ks for the RGS1. Using these good time intervals, we reprocessed the RGS1 data to produce the data files required for spectral analysis; i.e., the response matrix, the background spectrum, and the file containing the spectrum of H 2356-309 (which also contains background). We restrict our analysis to the first-order spectra, because the second order does not cover the relevant O VII line energies and its count rate is much lower.

*Chandra* observed H 2356-309 for 95.5 ks with the Low-Energy Transmission Grating (LETG) and the HRC-S detectors, which offer the best compromise between sensitivity and spectral resolution in the wavelength range of the O VII lines. We reduced the data using the standard *Chandra* Interactive Analysis of Observations (CIAO) software (v4.0) and *Chandra* Calibration Database (CALDB, v3.4.0) and followed the standard *Chandra* data reduction threads<sup>7</sup>. To ensure up-to-date calibration, we reprocessed the data from the “level 1” events file to create a new “level 2” file for analysis. We applied the latest HRC gain map and pulse-height filter for use with LETG data<sup>8</sup>. This procedure removed a sizable portion of background events with negligible X-ray event loss. From inspection of the light curves extracted from source-free regions of the detector, we concluded that the observation was not affected significantly by background flares.

We used the CIAO software to produce the files required for spectral analysis; i.e., the response matrix, the background spectrum, and the file containing the spectrum of H 2356-309 (which also contains background). Unlike the RGS, different orders cannot be separated from the LETG-HRC-S spectra, and so a given spectrum contains all orders. Consequently, by default we use a response matrix that includes information up to the sixth order. In §3.5 we compare results using a response matrix that includes information only on the first-order spectrum.

We re-binned the spectra to optimize detection of the absorption lines. After some experimentation, we achieved this by requiring a minimum of 75 and 40 counts per bin respectively in the RGS1 and LETG spectra.

In Figure 2 we present the background-subtracted *Chandra* and *XMM* spectra. (The background subtraction is achieved in the normal way in xspec via the “data”

<sup>6</sup> <http://xmm.esac.esa.int/sas/8.0.0/>

<sup>7</sup> <http://cxc.harvard.edu/ciao/threads/>

<sup>8</sup> <http://cxc.harvard.edu/contrib/letg/GainFilter/>

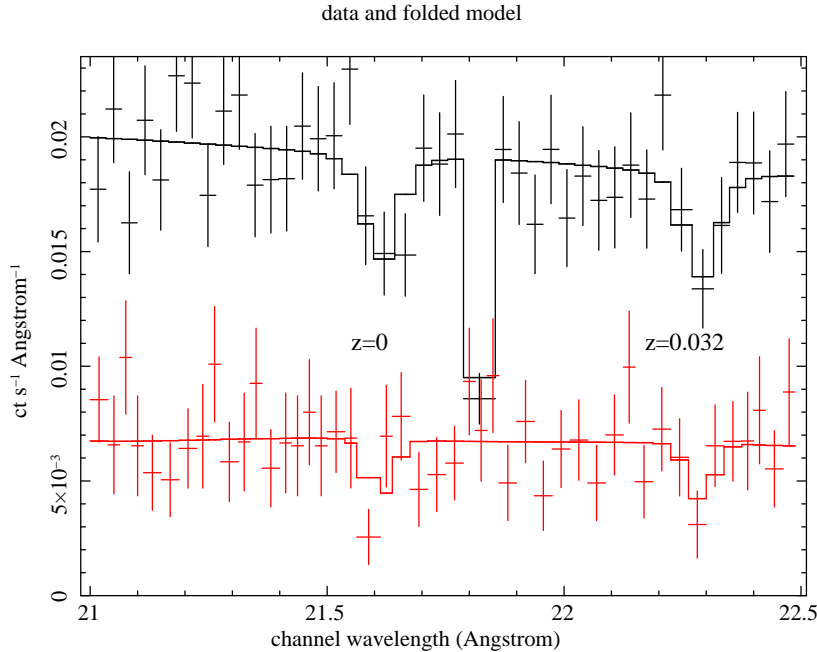


FIG. 2.— Background-subtracted *XMM* (black) and *Chandra* (red) spectra of the blazar H 2356-309 over the wavelength range 21.0–22.5 Å used to study the candidate O VII lines. The spectral models represent a power-law continuum, two absorption lines broadened by the instrumental resolution and the Voigt function, and foreground Galactic absorption from cold gas. The wavelength positions of the two absorption lines, nearby and Sculptor, are indicated.

and "backrnd" commands.) Two candidate absorption lines in each detector are immediately apparent upon visual inspection. The line near 21.6 Å corresponds to O VII for  $z = 0$ , consistent with nearby WHIM in the Local Group or hot gas in the Milky Way. However, the other candidate line near 22.3 Å corresponds to O VII for  $z \approx 0.03$ , consistent with the redshift of the unvirialized structure in the Sculptor Wall. (The absorption line near 21.8 Å in the RGS1 is a known instrumental feature.)

### 3. SPECTRAL FITTING

We performed spectral fitting using XSPEC v11.3.2ag (Arnaud 1996) and minimized the Cash C-statistic (Cash 1979), rather than  $\chi^2$ , to obtain unbiased parameter estimates from the Poisson-distributed spectral data (Humphrey et al. 2008). In all the fits the foreground absorbing Hydrogen column density from cold gas in the Milky Way was fixed at the value ( $1.33 \times 10^{20} \text{ cm}^{-2}$ ; Dickey & Lockman 1990) using the PHABS model in XSPEC.

#### 3.1. Models

A common practice in X-ray studies of the WHIM is to characterize the properties of a candidate absorption line by subtracting a gaussian component from a model of the continuum. The equivalent width is computed from this composite model, from which the column density of the absorber is inferred. This procedure is well suited to the case where the absorber is optically thin (i.e., linear part of the curve of growth), which we show is not the case for the candidate Galactic and extra-galactic WHIM absorbers in H 2356-309. In these cases a composite continuum-minus-gaussian model takes negative values at the line centers. Consequently, we constructed a physical line absorption model as follows.

Let  $I(E; 0)$  be the monochromatic specific intensity of photon energy  $E$  incident at coordinate  $s = 0$  assuming plane-parallel geometry. The emergent radiation at coordinate  $s$  is then,

$$I(E; s) = I(E; 0)e^{-\tau(E; s)}, \quad (1)$$

where the optical depth<sup>9</sup> is,

$$\tau(E; s) = N(s) \frac{\pi e^2}{m_e c} f \phi(E). \quad (2)$$

The quantity,  $N(s) = \int_0^s n ds$ , is the column density of absorbing atoms, and  $f$  is the absorption oscillator strength of the spectral line transition. The line-profile function,

$$\phi(E) = \frac{h}{\Delta E_D \sqrt{\pi}} H(a, u), \quad (3)$$

is expressed in terms of the Doppler width,

$$\Delta E_D = E_0 \frac{b}{c}, \quad (4)$$

where  $E_0$  is the rest-frame energy of the line, and

$$b = \sqrt{\frac{2k_B T}{m}} = 32.24 \sqrt{\frac{T}{10^6 \text{K}}} \frac{16}{A} \frac{\text{km}}{\text{s}}, \quad (5)$$

is the Doppler  $b$ -parameter. We have expressed  $b$  in terms of an oxygen atom of 16 atomic mass units. The quantity

<sup>9</sup> We do not correct for stimulated emission because (1) the effect is small for the resonance O VII line for expected WHIM temperatures, (2) the WHIM temperature is not precisely determined by our fits, and (3) the  $(1 - \exp[-E/K_B T])$  correction term applies assuming a thermal plasma, which may not be strictly valid for the WHIM.

$H(a, u)$  is the Voigt function which combines the effects of natural and Doppler broadening through the parameters,

$$a = \frac{h\Gamma}{4\pi\Delta E_D}, \quad u = \frac{\Delta E}{\Delta E_D}, \quad (6)$$

where,  $\Gamma$  is the Einstein-A coefficient of the line transition, and  $\Delta E = E - E_0$ . We used the implementation of the Voigt function provided by Wells (1999)<sup>10</sup>. We implemented the line absorption as a local multiplicative model in XSPEC, such that for a given energy bin of an input response matrix we evaluated the average of  $\exp[-\tau(E; s)]$  over 10 equally spaced energies within the bin. (The variation of  $I(E; 0)$  over an energy bin in the RGS and LETG response matrices is negligible.) For the resonance O VII  $K\alpha$  line we used  $E_0 = 0.574$  keV (21.6 Å),  $f = 0.696$ , and  $\Gamma = 3.3 \times 10^{12} \text{ s}^{-1}$  (Verner et al. 1996).

We find that a power-law model is a good description of the continuum over 21.0–22.5 Å (0.5515–0.5909 keV) in both *Chandra* and *XMM*. Both the photon spectral index and the normalization are fitted separately for each detector. Two absorption lines, one near  $z = 0$  and another near  $z = 0.03$ , were added following the above prescription. We required the parameters of the absorption lines to be the same in both detectors. Therefore, the model that we fitted to the data consists of a power-law continuum, two absorption lines, and (fixed) foreground Galactic absorption from cold gas.

### 3.2. Continuum

Upon fitting the composite model simultaneously to the *XMM* and *Chandra* spectra we obtain a spectral index of  $3.3 \pm 1.7$  and a 21.0–22.5 Å flux of  $(7.76 \pm 0.26) \times 10^{-13} \text{ erg cm}^{-2} \text{ s}^{-1}$  (unabsorbed) for the power-law continuum of the *XMM* spectrum (90% errors quoted for both quantities). Because the *Chandra* LETG–HRC–S spectrum contains photons from all orders, not just the first order, some photons with wavelengths smaller than 21.0 Å in the higher-order spectrum will be mis-classified as having wavelengths between 21.0–22.5 Å if the response matrix only includes information on the first-order diffraction spectrum. To account for the higher orders, the response matrix (§2) requires the spectral model to be defined down to wavelengths as small as  $\sim 5$  Å.

We adopted the following procedure to define the continuum for the *Chandra* data as a compromise between the desire to insure an accurate modeling of photons from higher orders and to measure the continuum using only data very close to the energies of the absorption lines. We initially fitted the power-law model modified by foreground Galactic absorption from cold gas to the background-subtracted *Chandra* data over the broad wavelength range 5–30 Å. This model provides a very good fit to the *Chandra* spectrum with a well-constrained power-law index,  $1.883 \pm 0.034$ . In all subsequent fits (though see §3.5) to the narrow band (21.0–22.5 Å) we restrict the power-law index for the *Chandra* data to lie between these values established by the broad-band fit, thereby insuring an accurate modeling of the

broad-band spectrum and thus the contribution from the higher orders. After fitting the composite model (i.e., continuum, absorption lines, foreground cold absorber) simultaneously to the *XMM* and *Chandra* spectra we obtain a 21.0–22.5 Å flux of  $5.52^{+0.39}_{-0.46} \times 10^{-13} \text{ erg cm}^{-2} \text{ s}^{-1}$  (unabsorbed) for the *Chandra* power-law continuum; i.e, the continuum flux of the blazar measured by *XMM* is about 40% higher than observed by *Chandra* over the spectral region of study.

### 3.3. Background

Over 21.0–22.5 Å the background comprises about 8% of the observed *XMM* count rate and about 38% of the *Chandra* count rate. As noted above, we perform spectral fitting on the background-subtracted *XMM* and *Chandra* spectra of the blazar. However, below in §3.4 we also assess the statistical significance of the O VII absorption lines using simulated spectra, for which we prefer to use model representations of both the source and background spectra for each satellite. We constructed models of the background spectra as follows.

The *Chandra* LETG–HRC–S background spectrum over 5–30 Å is fairly well described by a broken power-law folded through only the instrument RMF (“redistribution matrix file”) and not the ARF (“auxiliary response file”). This is achieved by defining a “BKNPOW/b” model in XSPEC v11. The model parameters are very tightly constrained. For reference, the best-fitting values for the power-law indexes are, 1.552 and 1.888, and the best-fitting break energy is, 1.338 keV (9.27 Å). Because the model is not a perfect fit to the data at all wavelengths, we adjusted the flux of the power-law to best match the spectral region of the oxygen lines. That is, adopting the values of the spectral indexes and break energy obtained from the broad-band fit we refitted the background model over the restricted range 21.0–22.5 Å of interest, which yields a normalization that is  $4\% \pm 2\%$  ( $1\sigma$ ) less than obtained for the broad-band fit.

For the *XMM* RGS1 the broad-band spectrum is not well described by simple models. Consequently, we adopted a single power-law model, again folded only through the RMF (“POW/b” model in XSPEC v11), but over a narrower wavelength region where the model is a good fit. We selected the wavelength range, 20–24 Å, as the largest range producing a good fit while enclosing the critical 21.0–22.5 Å interval. We obtain a power-law spectral index of 1.16 with a 90% confidence range (0.27–3.65).

### 3.4. Absorption Lines

In this section we discuss the significance and properties of the absorption lines obtained from fitting the composite model to the data, while systematic errors in our analysis are examined in §3.5.

We list in Table 1 the redshifts of the two candidate O VII  $K\alpha$  absorption lines obtained from fitting the spectral model simultaneously to the *XMM* and *Chandra* data. The line near 21.6 Å is fully consistent with hot gas from the Milky Way (or Local Group WHIM), with the inferred error range on the redshift being consistent with zero. The redshift range of the line near 22.3 Å

<sup>10</sup> <http://www.atm.ox.ac.uk/user/wells/voigt.html>

TABLE 1  
O VII SPECTRAL LINE PROPERTIES

	Redshift	$N$ ( $10^{16} \text{ cm}^{-2}$ )	$\tau_0$
Milky Way	-0.0004 - 0.0020	(5.5, 0.9)	(20.3, 2.2)
Sculptor	0.0311 - 0.0327	(4.7, 1.0)	(18.7, 2.1)

NOTE. — All parameters are quoted at the 90% confidence level. The redshift ranges are determined by allowing the Doppler  $b$ -parameter to take any value between 1-300 km/s, a large range that should bracket physical WHIM values, and the redshifts themselves were allowed to take any values during the fits. The column densities and line-center optical depths are lower limits evaluated assuming two values for the  $b$ -parameter (50, 100) km/s.

matches very well the range of structure in the Sculptor Wall ( $z = 0.028 - 0.032$ ) that intercepts the blazar’s line-of-sight. Henceforth, we refer to these candidate lines as the Galactic and Sculptor WHIM lines.

The change in the fit statistic, whether it be the C-statistic or  $\chi^2$ , is very similar when adding the Galactic and Sculptor WHIM lines, indicating that the statistical significance of the lines is also similar. For reference, the change in the  $\chi^2$  statistic observed when adding the Sculptor WHIM line to the fit suggests the line is significant at the  $\approx 3\sigma$  level when interpreted in terms of the F-Test. However, the F-Test is not strictly applicable to spectral line detection (Protassov et al. 2002).

To obtain a rigorous estimate of the statistical significance of the Sculptor WHIM line we employed a Monte Carlo procedure. Using as a reference the best-fitting spectral model excluding the Sculptor WHIM line, we generated with XSPEC synthetic *XMM* and *Chandra* spectra for the source and background (§3.3) with the same exposure times as the real data. The simulations were performed using the full energy resolution of the response matrices, after which the synthetic spectra were re-grouped as described in §2. In this way the simulations account for noise associated with the re-binning procedure.

We fitted the synthetic background-subtracted spectra with the reference model and minimized the C-statistic to obtain a best fit. Then we added a second absorption line component *with redshift range restricted to 0.028-0.032* appropriate for the Sculptor Wall. After obtaining the new best fit, we recorded the reduction in the C-statistic. We performed this procedure for  $10^4$  simulations. The probability of a false detection is given by the number of simulations where the reduction in the C-statistic is at least as large as observed in the real fit relative to the total number of simulations.

The fit of the reference model (i.e., without the Sculptor WHIM line) to the real data yields a best-fitting value of the C-statistic of 68.2 for a total of 88 spectral bins. Upon adding the Sculptor line and re-fitting, we obtain a C-statistic of 58.6 for a reduction of 9.6. For the Monte Carlo procedure described above, we find that in only 36 out of the  $10^4$  simulations is the C-statistic reduced by at least 9.6. This translates to a false detection probability of 0.36%. Therefore, the statistical significance of the Sculptor WHIM line is 99.64%; i.e., about  $3\sigma$ . Following the same procedure, but this time starting without the Milky Way line and with the Sculptor WHIM line already in place, we determine the statistical significance of the Milky Way line to be 99.69%, also about  $3\sigma$ .

(We mention that the *XMM* data contribute more to the statistical significance than do the *Chandra* data. If the spectral fitting is performed separately for each data set, then following the above Monte Carlo procedure for the Sculptor WHIM line we obtain a statistical significance of  $2.4\sigma$  for *XMM* and  $1.7\sigma$  for *Chandra*.)

Apart from the redshift noted above, the line parameters are not well constrained by the data. In Table 1 we list the 90% confidence lower limits obtained for the O VII  $K\alpha$  column density ( $N$ ) and line-center optical depth ( $\tau_0 = \tau(E_0, s)$ ). We quote results for two values of the  $b$ -parameter (50, 100)  $\text{km s}^{-1}$  which span a large range of WHIM temperature and turbulent pressure.

The lower limits of  $\tau_0 \approx 1$  for both lines demonstrate that the line centers are not optically thin. Therefore, one cannot infer the column density from the equivalent width independent of the  $b$ -parameter; i.e., these lines do not lie on the linear portion of the curve of growth. For reference, the best-fitting equivalent widths are nearly 30 mÅ for both the Galactic and Sculptor lines.

The column density lower limits of  $\approx 10^{16} \text{ cm}^{-2}$  are consistent with expectations for both lines. Similar column densities previously have been reported for the Milky Way (or Local Group WHIM) (e.g., Fang et al. 2003). As for the Sculptor line, we re-examined the cosmological hydrodynamical simulation of Cen & Fang (2006) and identified five super-structures with similar (or higher) galaxy over-density relative to the Sculptor Wall. By shooting random sight-lines through these super-structures we obtain a mean O VII column density of  $\approx 3 \times 10^{16} \text{ cm}^{-2}$ , consistent with the limits imposed by our spectral fits on the Sculptor Wall.

### 3.5. Systematic Errors

The large statistical errors obtained for the line column densities and line-center optical depths dominate systematic errors associated with our data analysis and modeling choices, and therefore we do not provide a detailed systematic error budget for the line parameters. However, in this section we briefly discuss the possible impact of systematic errors on the estimation of the significance of the Sculptor Wall WHIM line, which is the principal result of our paper. We have in particular considered the effects of errors in the background models and the wavelength calibration of the detectors, and we have also examined using  $\chi^2$  rather than the C-statistic.

As we mentioned in §3.3, the background level is only a small fraction of the total observed flux for the *XMM* RGS. Consequently, it is expected that small variations in the background level from that we adopted in our fits should have little effect on the significance estimate. Indeed, varying the background level by  $\pm 5\%$ , which reflects the statistical error on the power-law model obtained for the RGS background, did not have a noticeable effect.

Because the *Chandra* LETG-HRC-S is unable to separate spectra of different orders, we examined how much our results change if instead we used a response matrix containing only information on the first-order spectrum. Using only the first-order response leads to an underestimation of the actual background by almost 20% over the 21.0 – 22.5 Å range. Since the first-order response does not require a valid continuum model outside our range

of interest, we allowed the slope of the continuum to be fitted without restriction over 21.0 – 22.5 Å, which provides a measure of the sensitivity of the results to the definition of the continuum. When performing simultaneous RGS-LETG fits using the first-order response for the LETG we obtain a statistical significance of the Sculptor WHIM line of 99.53%, only slightly less than obtained when using the more accurate response containing orders 1 through 6.

We also considered systematic uncertainties in the wavelength calibration of the detectors. Current estimates indicate the calibrations are accurate to within 2.4 mÅ in the RGS1<sup>11</sup> and to 10 mÅ in the LETG/HRC-S<sup>12</sup>. We find little difference in any of our results when allowing for shifts of these magnitudes between the detectors. We do mention that if the wavelength of the  $z = 0$  line is allowed to be fitted separately for the RGS1 and the LETG then the best-fitting line centers are offset by 48 mÅ. However, the shift is significant only at the  $\sim 90\%$  confidence level, and it is substantially larger than the expected calibration uncertainty, indicating this marginal shift is probably noise. Therefore, we kept the line energies tied between the detectors.

Finally, we also performed all of our fits by minimizing (data-weighted)  $\chi^2$  and obtained a consistent result for the significance of the Sculptor line as obtained using the C-statistic. In particular, the statistical significance of the Sculptor line obtained using  $\chi^2$  is, 99.81%, about  $3\sigma$ .

#### 4. CONCLUSIONS

We report a detection at the  $3\sigma$  level of an O VII  $K\alpha$  resonance absorption line located in the Sculptor Wall super-structure of galaxies. The column density ( $\gtrsim 10^{16} \text{ cm}^{-2}$ ) of the line, though not precisely constrained, is consistent with that produced by similar structures generated in cosmological simulations. The presence of this absorption line is inferred from simultaneous analysis of *XMM* RGS1 and *Chandra* LETG/HRC-S spectra of the blazar H 2356-309 ( $z = 0.165$ ). Since the line center is saturated (for both the Sculptor and Local lines), we interpreted the spectra with a physical model where the line is modified by the Voigt profile to account for both natural and Doppler broadening.

<sup>11</sup> A. Pollock, XMM-Newton Users Group Meeting Presentations, 6-7 May 2008, [http://xmm.esac.esa.int/external/xmm\\_user\\_support/usersgroup/20080506/](http://xmm.esac.esa.int/external/xmm_user_support/usersgroup/20080506/)

<sup>12</sup> M. Chung et al., <http://cxc.harvard.edu/cal/Letg/Corrlam/>

The robustness of the detection benefits from three key aspects of our study. First, a critical factor in obtaining this high detection significance level is that we know *a priori* the redshift of the intervening structure in the Sculptor Wall ( $z = 0.028 - 0.032$ ). The importance of this point was dramatized in the controversy over the claimed WHIM detection in the spectrum of Mrk 421 (Nicastro et al. 2005; Kaastra et al. 2006). Second, the line is detected from a joint analysis of *XMM* and *Chandra* data. The consistent picture from the two satellites provides important reassurance given again the controversy for Mrk 421 where the RGS did not confirm the claimed *Chandra* detection (Rasmussen et al. 2007). Third, since the background source is a blazar, it is very unlikely that features intrinsic to the source contaminate our study of the foreground WHIM.

This detection of WHIM in the Sculptor Wall represents the most significant (non-local) WHIM detection to date from X-ray absorption studies, providing vital evidence for the expected repository of the “missing baryons” (e.g., Fukugita et al. 1998; Cen & Ostriker 1999; Davé et al. 2001) complementary to that of X-ray emission studies of WHIM in superclusters (e.g., Zappacosta et al. 2005) and the intersections of binary clusters (e.g., Werner et al. 2008), and O VI absorption line studies that probe WHIM at lower temperatures (e.g., Savage et al. 1998; Tripp et al. 2006).

We thank the referee for re-analyzing the *XMM* data and verifying our result. D.A.B., T.F, and P.J.H. gratefully acknowledge partial support from NASA through Chandra Award Numbers GO7-8140X issued by the Chandra X-ray Observatory Center, which is operated by the Smithsonian Astrophysical Observatory for and on behalf of NASA under contract NAS8-03060. We also are grateful for partial support from NASA-XMM grant NNX07AT24G. We thank Dr. R. Remillard for providing daily RXTE fluxes for H 2356-309. This research has made use of the NASA/IPAC Extragalactic Database (NED) which is operated by the Jet Propulsion Laboratory, California Institute of Technology, under contract with the National Aeronautics and Space Administration.

#### REFERENCES

- Arnaud, K. A. 1996, in *Astronomical Society of the Pacific Conference Series*, Vol. 101, *Astronomical Data Analysis Software and Systems V*, ed. G. H. Jacoby & J. Barnes, 17
- Cash, W. 1979, *ApJ*, 228, 939
- Cen, R. & Fang, T. 2006, *ApJ*, 650, 573
- Cen, R. & Ostriker, J. P. 1999, *ApJ*, 514, 1
- da Costa, L. N., Geller, M. J., Pellegrini, P. S., Latham, D. W., Fairall, A. P., Marzke, R. O., Willmer, C. N. A., Huchra, J. P., Calderon, J. H., Ramella, M., & Kurtz, M. J. 1994, *ApJ*, 424, L1
- Davé, R., Cen, R., Ostriker, J. P., Bryan, G. L., Hernquist, L., Katz, N., Weinberg, D. H., Norman, M. L., & O’Shea, B. 2001, *ApJ*, 552, 473
- Dickey, J. M. & Lockman, F. J. 1990, *ARA&A*, 28, 215
- Fang, T., Sembach, K. R., & Canizares, C. R. 2003, *ApJ*, 586, L49
- Fujimoto, R., Takei, Y., Tamura, T., Mitsuda, K., Yamasaki, N. Y., Shibata, R., Ohashi, T., Ota, N., Audley, M. D., Kelley, R. L., & Kilbourne, C. A. 2004, *PASJ*, 56, L29
- Fukugita, M., Hogan, C. J., & Peebles, P. J. E. 1998, *ApJ*, 503, 518
- Humphrey, P. J., Liu, W., & Buote, D. A. 2008, *ApJ*, accepted (arXiv:0811.2796)
- Kaastra, J. S., Werner, N., Herder, J. W. A. d., Paerels, F. B. S., de Plaa, J., Rasmussen, A. P., & de Vries, C. P. 2006, *ApJ*, 652, 189
- Kravtsov, A. V., Klypin, A., & Hoffman, Y. 2002, *ApJ*, 571, 563
- Nicastro, F., Mathur, S., Elvis, M., Drake, J., Fiore, F., Fang, T., Fruscione, A., Krongold, Y., Marshall, H., & Williams, R. 2005, *ApJ*, 629, 700

- Protassov, R., van Dyk, D. A., Connors, A., Kashyap, V. L., & Siemiginowska, A. 2002, *ApJ*, 571, 545
- Rasmussen, A. P., Kahn, S. M., Paerels, F., Herder, J. W. d., Kaastra, J., & de Vries, C. 2007, *ApJ*, 656, 129
- Richter, P., Paerels, F. B. S., & Kaastra, J. S. 2008, *Space Science Reviews*, 134, 25
- Savage, B. D., Tripp, T. M., & Lu, L. 1998, *AJ*, 115, 436
- Tripp, T. M., Bowen, D. V., Sembach, K. R., Jenkins, E. B., Savage, B. D., & Richter, P. 2006, in *Astronomical Society of the Pacific Conference Series*, Vol. 348, *Astrophysics in the Far Ultraviolet: Five Years of Discovery with FUSE*, ed. G. Sonneborn, H. W. Moos, & B.-G. Andersson, 341–+
- Verner, D. A., Verner, E. M., & Ferland, G. J. 1996, *Atomic Data and Nuclear Data Tables*, 64, 1
- Wells, R. J. 1999, *J. Quant. Spectrosc. Radiat. Transfer*, 62, 29
- Werner, N., Finoguenov, A., Kaastra, J. S., Simionescu, A., Dietrich, J. P., Vink, J., & Böhringer, H. 2008, *A&A*, 482, L29
- Zappacosta, L., Maiolino, R., Mannucci, F., Gilli, R., & Schuecker, P. 2005, *MNRAS*, 357, 929
- Zappacosta, L., Mannucci, F., Maiolino, R., Gilli, R., Ferrara, A., Finoguenov, A., Nagar, N. M., & Axon, D. J. 2002, *A&A*, 394, 7